Research Article | Vol. 30, No. 12 / 6 Jun 2022 / Optics Express 21833
Optics EXPRESS

Low bending loss few-mode hollow-core anti-resonant fiber with glass-sheet conjoined nested tubes

HUABEI LIU,[1] YU WANG,[1,2] YAN ZHOU,[1,4] ZUGUANG GUAN,[1] ZHANGWEI YU,[1] QIANG LING,[1] SI LUO,[1] JIE SHAO,[1] DONGMEI HUANG,[3] AND DARU CHEN[1,5]

[1]*Hangzhou Institute of Advanced Studies, Zhejiang Normal University, Hangzhou 311231, China*
[2]*Photonics Research Centre, Department of Electronic and Information Engineering, The Hong Kong Polytechnic University, Hung Hom, Kowloon, Hong Kong, China*
[3]*Photonics Research Centre, Department of Electrical Engineering, The Hong Kong Polytechnic University, Hong Kong SAR, China*
[4]*zy9410@zjnu.edu.cn*
[5]*daru@zjnu.cn*

Abstract: A novel hollow-core anti-resonant fiber (HC-ARF) with glass-sheet conjoined nested tubes that supports five core modes of LP01-LP31 with low mode couplings, large differential group delays (DGDs), and low bending losses (BLs) is proposed. A novel cladding structure with glass-sheet conjoined nested tubes (CNT) is induced for the proposed HC-ARF which can suppress mode couplings between the LP01-LP31 modes and the cladding modes. The higher-order modes (HOMs) which are LP11-LP31 modes also have very low loss by optimizing the radius of the nested tube and the core radius. Moreover, the large effective refractive index differences Δn_{eff} between HOMs are all larger than 1×10^{-4} which contributes to a large DGD in the wavelength range from 1.3 to 1.7 μm. The bending loss of the HC-ARF is analyzed and optimized emphatically. Our calculation results show that bending losses of LP01-LP31 modes are all lower than 3.0×10^{-4} dB/m in the wavelength range from 1.4 to 1.61 μm even when the fiber bending radius of the HC-ARF is 6 cm.

1. Introduction

Hollow-core fibers (HCFs) have attracted tremendous interest of many research groups in the past decades due to their advantages of low scattering and weak nonlinearity since the light is guided in the air core [1–4]. Many types of optical fibers have been proposed one after another, such as hollow-core Bragg fiber [5], hollow-core photonic crystal fiber (HC-PCF) [6], kagome fiber [7] and hollow-core anti-resonant fiber (HC-ARF) [8–11]. The HC-ARF is mainly composed of a circle of negative curvature tubes. Due to the special working mechanism, the confinement loss (CL) and bending loss (BL) are much bigger than the surface scattering loss (SSL) which become the main losses [12]. Anti-resonance is the prerequisite for inhibiting core-cladding modes coupling and bring some remarkable transmission properties such as wide bandwidth. A wavenumber mismatch between the core and the cladding modes inhibits coupling between the modes and leads to remarkably low loss [13]. In the early research of the HC-ARF with a simple structure such as a single round glass tube, the loss is much higher compared with traditional silica core fiber [14]. In order to further reduce the transmission loss, novel HC-ARFs have been proposed such as nodeless cladding tube and nested cladding tube [15–17]. In 2019, Bradley. T, *et al* reported the fabrication of a nested anti-resonant nodeless hollow-core fiber (NANF) with a minimum loss of 1.3 dB/km at 1450 nm and a 65 nm bandwidth below 1.5 dB/km [18]. In 2020, Jasion, G. T., *et al* reported an effective single-mode, 1.7 km long hollow core NANF

#446841 https://doi.org/10.1364/OE.446841
Journal © 2022 Received 7 Dec 2021; revised 13 Mar 2022; accepted 24 Mar 2022; published 2 Jun 2022

Optics EXPRESS

with a record-low loss 0.28 dB/km from 1510 to 1600 nm [19]. However, in previous reports, only the low transmission loss for the fundamental mode was achieved and investigated for the single-mode ARFs.

The spatial division multiplexing (SDM) technology is widely applied to increase the optical communication capacity [20] by using multiple distinguishable spatial information channels in the same multimode fiber core [21,22]. Few-mode fiber and SDM technology are integrated with each other to increase the link density. However, the application of the SDM technology is restricted by the mode coupling of the few-mode fiber. An effective way to solve this problem is to design a non-coupling few-mode fiber in which the effective index difference Δn_{eff} between the guided modes is $>1.0 \times 10^{-4}$ [23]. The process of HC-ARF offers the possibility to break this limitation [24,25]. Hollow-core conjoined-tube ARF(CTF) was reported in 2018 [26]. This new CTF combines almost all the qualities: ultralow transmission loss (2 dB/km), wide bandwidth and low BL. In 2020, Z. Wang *et al.* proposed a dual-mode weakly coupled anti-resonant fiber, which allowed LP01 and LP11 mode guided in the core [17]. The same year, A low loss, large bandwidth HC-ARF design for short-reach links was present by W. Shere *et al.* [27]. So a few-mode HC-ARF which can support several low-loss guiding modes without non-coupling is highly appreciated for applications of the SDM technology in optical communications.

In this paper, we design a novel HC-ARF with glass-sheet conjoined nested tubes cladding structure, and systematically study how to realize the low transmission loss of the few-mode guiding with low mode couplings, large DGDs and low BLs. The size of nested tube and core radius are strictly optimized and chosen to meet the requirements for applications in optical communication that the loss is $<3.0 \times 10^{-4}$ dB/m and DGDs are $\gg$0.1 ps/m [28]. In addition, the BL and bandwidth of HOMs is further analyzed and demonstrated by using optimized nested tube. Simulated results show that the few-mode fiber can meet the low-loss requirements in the wavelength range of 1.4-1.61 μm even when the bending radius is 6 cm.

2. Fiber structure

The cladding structure of CNT is shown in Fig. 1(a). The thickness t of the cladding glass tubes and sheet is determined by the anti-resonance relationship [13]:

$$t = \frac{\lambda(m - 0.5)}{2\sqrt{n^2 - 1}} \tag{1}$$

Where λ is the wavelength, and the effective refractive index value n of the glass is 1.444 for the wavelength of 1.55 μm. We choose anti-resonance order m=2 to both keep low loss and satisfy the fabrication feasibility [17], which results to t=1.12 μm. R and d are the core and cladding tubes radius, and g is the gap between the cladding tubes. The three parameters satisfy the geometric relationship:

$$d = \frac{g/2 - R\sin(\pi/k)}{\sin(\pi/k) - 1} \tag{2}$$

where k is the number of cladding tubes and we set k = 6, which has larger low loss bandwidth compared with other numbers [12].

A HC-ARF with a non-conjoined nested tube (NCNT) structure is shown in Fig. 1(b), which provides a compared investigation in details for how the proposed few-mode HC-ARF achieves few-mode transmission. Note that there are only slight differences for the nested tubes in the structure of the two fibers, but there are huge differences in the few-mode property.

Optics EXPRESS

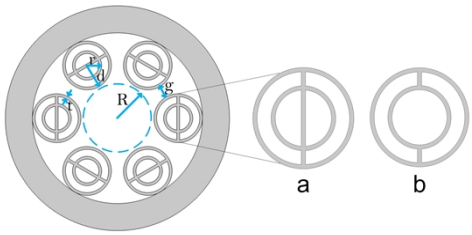

Fig. 1. Two different fiber cladding structures. (a) conjoined nested tube (CNT) and (b) non-conjoined nested tube (NCNT).

3. Optimization of few-mode HC-ARF supporting mode LP01-LP31

The simulation was conducted by a full finite element method, which numerically analyzes the mode characteristics of our proposed fibers. An optimized perfect matching layer (PML) is placed outside the cladding. The thickness is one tenth of the total thickness of the core and cladding for absorbing the leakage optical field. Very fine λ/4 and λ/6 grid sizes are used on the air and silica tubes respectively to ensure the convergence of the calculation results [25].

3.1. Effect of nested tube radius and gap on CL

Without loss of generality, R/λ is typical 10 to 20. We choose λ=1.55 μm and the core radius R = 15 μm [13]. The r/d is expressed the size of the conjoined nested tube in order to be consistent with the following description. Firstly, we discussed the effect of the structural parameters g on the CL of LP01. While we also scanned the r/d for convincing result. Figure 2 plots the thermal distribution of the LP01 CL when the r/d and g change, where Fig. 2(a) and Fig. 2(b) correspond to the NCNT and CNT structures, respectively. It is shown that the change in CL due to g is not almost affected by r/d. The lowest loss is around g = 1.5 μm on the horizontal axis. The design with a small g can eliminate Fano resonance caused by the nodes of connected cladding tubes [8]. However, the resonant tube cannot confine the light when g is too large [29]. An appropriate g must be set in advance since we focused on the effect of r/d in the following, so we set g = 1.5 and keep it the same.

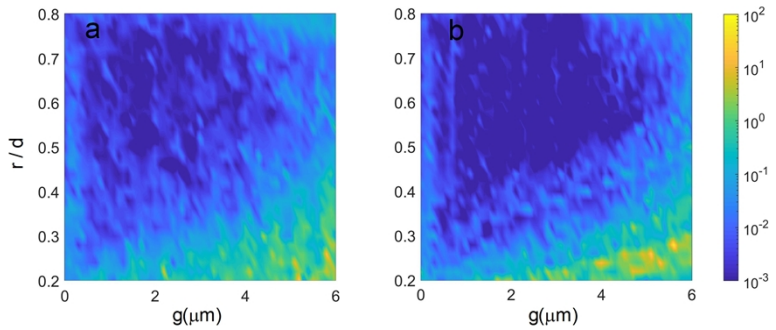

Fig. 2. The LP01 CL thermal distribution of parameters g and r/d. Fig. (a) and (b) correspond to the NCNT and CNT structures. The value from small to large corresponds to the color from blue to yellow.

3.2. Effect of CNT structure on HOMs

According to the former discussions, the g is set as 1.5 μm, and the HOMs of the two structural fibers are simulated and analyzed. Figure 3 shows the simulation results of core mode LP01-LP31

Optics EXPRESS

and main cladding modes (NCNT01, NCNT11, CNT01). The CLs of the LP01-LP31 modes decrease rapidly when the r/d increases from 0.2 to 0.4 since larger nested tube increases the light-confining ability of the cladding no matter NCNT or CNT structural. CL curves of LP01 and LP11 modes are still relatively stable and the value are low when r/d range from 0.4 to 0.7. However, the CLs of LP21-LP31 show peaks for the NCNT structure at r/d = 0.55, 0.61 and 0.65, respectively, which is caused by the coupling between the cladding mode NCNT01 as shown in Fig. 3(b). Note that the mode of NCNT11 has never been coupled with core modes.

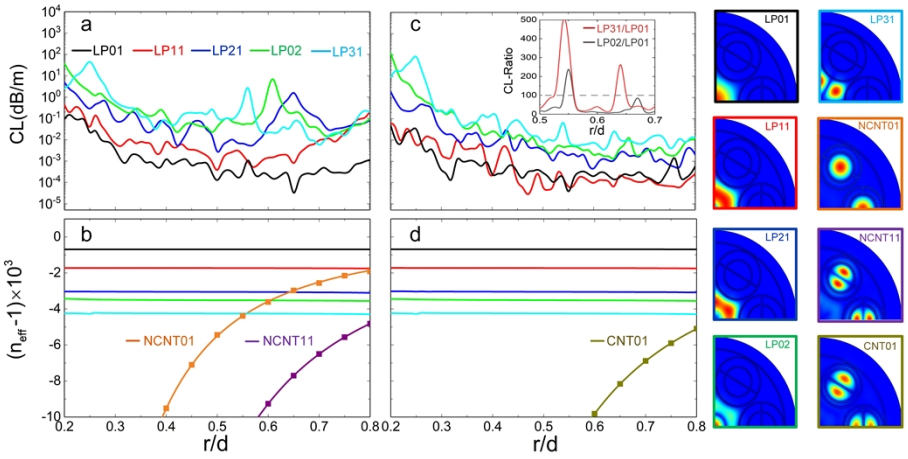

Fig. 3. Effect of changing r/d while the core radius R = 15 μm and g = 1.5 μm. (a) and (b) correspond to NCNT-ARF; (c) and (d) correspond to CNT-ARF. Tow CL-Ratios curves is plotted in inserted figure in Fig. 3(c). The solid squares are calculated values of cladding modes (NCNT01, NCNT11, CNT01). The color of the frame corresponds to the color of line of the plot.

We also calculated the n_{eff} of the cladding modes by the modified Marcatili- Schmeltzer mode [30]:

$$n_{lk} = 1 - \frac{1}{2}\left(\frac{u_{lk}\lambda}{2\pi fr}\right)^2 \tag{3}$$

where u_{lk} is the k-th zero solution of the Bessel function J_l, r is radius of the nested tube, and f is a fitting parameter. The f of cladding modes NCNT01, NCNT11 and CNT01 is 1.00472, 0.99509, 0.96635, respectively. The analysis results are shown as the solid curve in Fig. 3(b) and(d), which matches well with the simulation results of solid square.

Compared with NCNT structure, the loss peaks of the CNT structure don't show again as shown in Fig. 3(c), because the conjoined nested tube can directly eliminate the NCNT01 mode and the CNT01 mode equivalent to the NCNT11 mode has never been coupled with core modes as shown in Fig. 3(d). Moreover, the CL-Ratio curves of LP02/LP01 and LP31/LP01 as shown in the inserted figure in Fig. 3(c) all are 100 in the range of r/d= 0.56-0.63. And the average CLs of the LP01-LP31 modes are also the lowest in this range. A window is provided for exploring the low bending loss few-mode HC-ARF in the next. It is noted that the n_{eff} of the cladding modes changed drastically with the variation of the r/d, while the core modes kept relatively stable. The core modes and the cladding modes are independent, which is consistent with the analysis of the hollow core theory [30]. It provides a key way for us to decrease the loss by optimized r/d.

3.3. *Effect of core radius on few-mode of LP01-LP31*

In a few-mode fiber, the Δn_{eff} of adjacent modes should be $>10^{-4}$ to reduce modes crosstalk [23]. The core radius R is scanned from 14 to 25 μm while the r/d is fixed to 0.6. Simulation has been

Optics EXPRESS

carried out and the Δn_{eff} of adjacent modes with different R is plotted in Fig. 4(a), and each Δn_{eff} are $>10^{-4}$. The Δn_{eff} of LP02-LP21 modes is the smallest among the LP01- LP31 modes at different R, and the minimum values is 1.7×10^{-4} at R = 25 μm. In order to ensure the weak coupling between the modes, we did not further increase the radius.

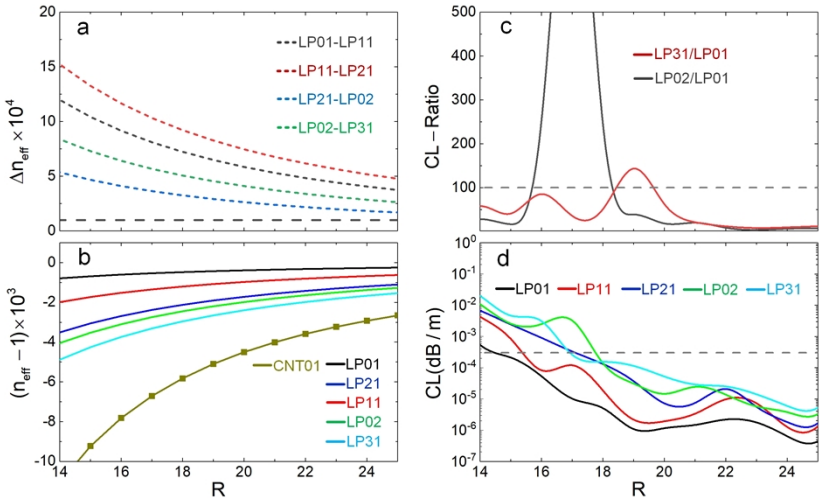

Fig. 4. Effect of changing core radius R with the r/d = 0.6 and g = 1.5μm. The gray dotted line in Fig.(a) (c) (d) are our expected baselines. In Fig.(b), the solid squares are simulated values of CNT01 mode, the dark yellow solid curve is calculated by Eq.3 with an f value of 0.96842 which agree well with the solid squares. The color of the frame corresponds to the color of line of the plot.

The above research shows that the HC-ARF can provide a possibility for few-mode transmission. And the CLs of core modes can be decreased by increasing core radius that meet the requirement in long-range optical communication [16]. The n_{eff} of the LP01-LP31 modes gradually increase and converge with increasing the core radius R as shown in Fig. 4(b). Although the CNT01 mode increases faster than the core modes, the CNT01 mode is not coupled with the LP01-LP31 modes. The CLs decrease as R increases and there is no obvious loss peak as shown in Fig. 4(d). The CLs of the LP01-LP31 modes all $<3.0 \times 10^{-4}$ dB/m in the range of R = 18-25 μm. In Fig. 4(c), we also plot CL-Ratios of the LP02/LP01 and LP31/LP01 in the range of R = 14-25 μm, and the value are <100 when R is greater than 20 for the two curves.

According to the above discussion, the core radius R not only has an important influence on CL, but also plays a decisive role in Δn_{eff} of adjacent modes. The LP01-LP31 modes always maintain low loss due to the structural characteristics of CNT. In order to effectively reduce the losses, CL ratio and weak mode coupling, the core radius R must be selected carefully.

3.4. *Transmission property of few-mode*

Based on the above analysis about the loss, CL-Ratio and modes coupling factors, we finally set the core radius R = 23 μm. We analyze the transmission property of CNT-ARF in the wavelength range of λ=1.3-1.7 μm. Figure 5(b) plots the Δn_{eff} curve of adjacent modes at different wavelength. The Δn_{eff} of LP02-LP21 modes with the smallest value has a minimum value of 1.43×10^{-4} at 1.3 μm. The DGDs of adjacent modes at different wavelength have been studied as shown in Fig. 5(a) which is a crucial feature to assess the performance of few-mode fibers [30]. The calculation result shows the trends of the four DGD curves all increase with wavelength, and the lowest curve of LP02-LP21 has a minimum value of 0.48ps/m at 1.3 μm. DGDs between five adjacent

Optics EXPRESS

modes is 1.48, 1.88, 0.67, 1.04 ps/m at 1.55 μm, respectively. As the value is ≫ 0.1 ps/m, the two guided modes are well separated.

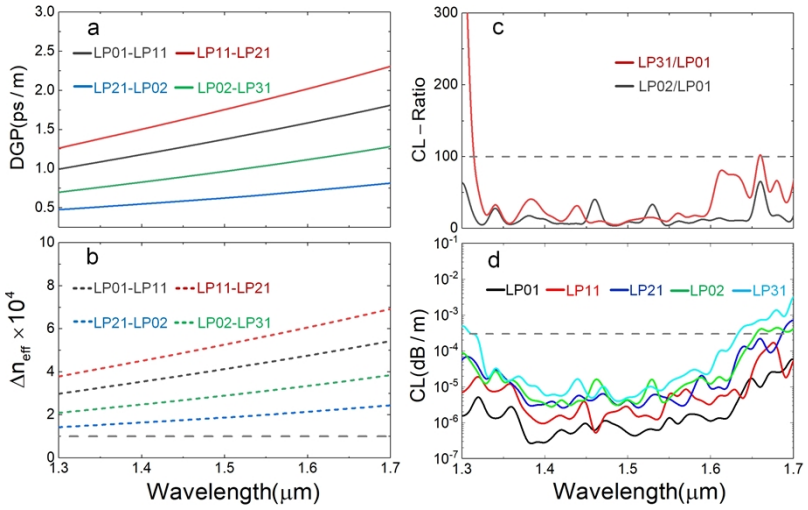

Fig. 5. Effect of changing wavelength while the r/d = 0.6, R = 23 and g = 1.5μm. The gray parallel line in Fig.(b) (c) (d) are our expected baselines. The color of the frame corresponds to the color of line of the plot.

The CLs and CL-Ratios of LP01-31 modes is very low as shown in Fig. 5(c) and (d). The anti-resonance condition can broaden the bandwidth, while the CNT structure reduces the losses in higher order modes. The CLs of LP01 and LP11 modes are much $<3.0 \times 10^{-4}$ dB/m in the whole band, and the CLs of LP21-LP31 modes is lower than this standard value at 1.33-1.63 μm. On the other hand, Fig. 5(c) shows that the CL-Ratio of LP02/LP01 is <100 in the range of λ=1.3-1.7 μm. And the CL-Ratio of LP31/LP01 is <100 in the range of λ=1.33-1.63 μm. In general, the optimized few-mode HC-ARF can support LP01-LP31 modes with low mode couplings, large DGDs and low CL in a large wavelength range of 1.33-1.63 μm.

4. Bending loss

4.1. Effect of bending

Bending has a great influence on the transmission of optical fibers, especially the hollow core fiber. The effect of bending on the fiber is studied by using a conformal mapping technique [31,32]. We mainly study the X direction as shown in Fig. 6(a), which is more sensitive to the bending than the Y since the easier coupling between core and cladding modes [15,17]. While the wavelength is set to 1.55 μm, g = 1.5 μm, R = 23 μm and r/d = 0.6. Figure 6(c) shows that BLs increases with the decrease of the bending radius. The BL exhibits a smooth trend when the bending radius is greater than 6 cm, where the maximum value is only 1.17×10^{-4} dB/m, and the values is 3.0×10^{-4} dB/m in LP01-LP31 modes. However, the BL increases significantly when the bending radius is less than 6 cm and the BL peaks of LP2 mode and LP31 mode appear at 3 cm and 4 cm, respectively, which is caused by the coupling of CNT01 mode, as shown in Fig. 6(d). The Δn_{eff} curves of adjacent modes at different bending radius are shown in Fig. 6(b). In the case of extremely bending, Δn_{eff} significantly increase as bending radius decrease. But there is almost no change in Δn_{eff} when the bend radius is greater than 6 cm. For example, the growth of Δn_{eff} of LP01-LP11 is around 1.1×10^{-5} at 6 cm.

We also analyzed the influence of bending on the bandwidth. Figure 7(a) and (b) plots the BLs and n_{eff} curves of LP01-LP31, respectively, in the range of λ=1.3-1.7 μm when the bending

Optics EXPRESS

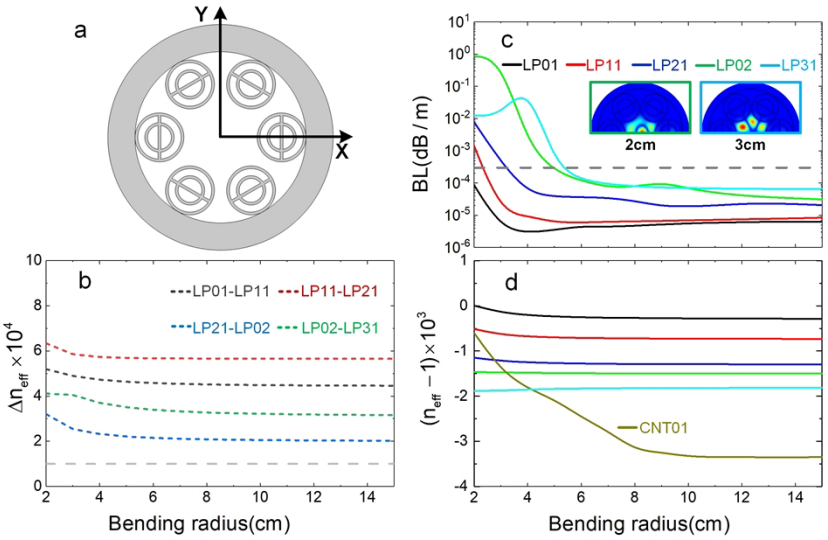

Fig. 6. Effect of bend while the r/d = 0.6, R = 23 μm, wavelength = 1.55 μm and g = 1.5 μm. The gray parallel line in Fig.(a) is our expected baselines. The color of the frame corresponds to the color of line of the plot.

radius is 6 cm. Figure 7(a) shows that the BLs of LP01 and LP11 modes are $<3.0 \times 10^{-4}$ dB/m in the wavelength range of λ=1.31-1.66 μm. The BL of the LP21 mode is also lower than the standard line within λ=1.32-1.66 μm. However, we can find that the LP02 mode and LP31 mode are coupled with CNT01 at wavelengths of 1.3 μm and 1.39 μm, respectively, as shown in Fig. 7(b), which results in high loss peaks. Therefore, the low loss range of LP02 and LP31 are shortened to 1.43-1.63 μm and 1.46-1.61 μm, respectively. The transmission bandwidth is greatly reduced compared with straight fiber.

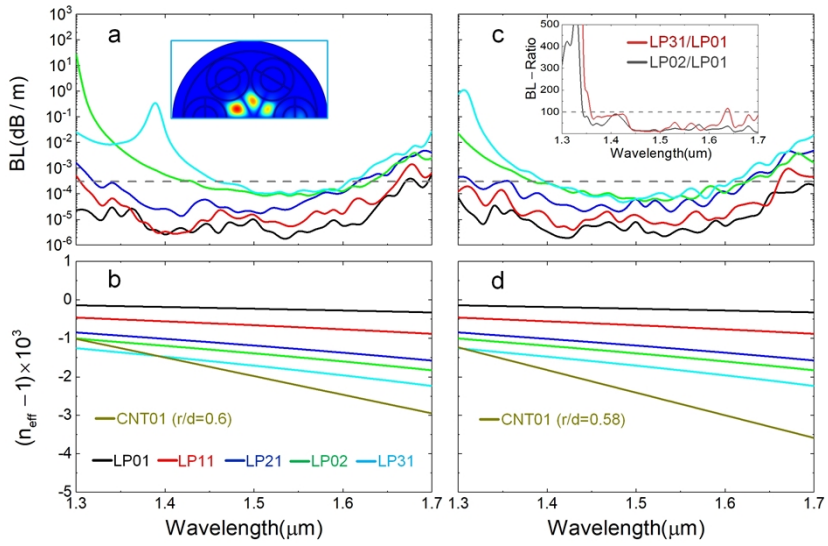

Fig. 7. Effect of bending on the bandwidth while the R = 23 μm, g = 1.5 μm. The gray parallel line in Fig.(a) (b) is our expected baselines. The color of the frame corresponds to the color of line of the plot.

Optics EXPRESS

4.2. Optimization of BLs

In order to expand the available bandwidth, more optimization and adjustment must be proposed to limit the coupling of LP02-LP31 and CNT01. According to our discussion in section 3.2, the n_{eff} of the CNT01 mode can be significantly changed by r/d while keeping the n_{eff} of the core modes unchanging. It can be seen from Fig. 7(b) that if the n_{eff} of CNT01 decreases, the coupling between cladding and core modes can be suppressed. According to Eq.3, the parameter r/d should be reduced to achieve this aim. We obtained the low-loss transmission window with r/d of 0.56-0.63 for the few-mode HC-ARF in section 3.2. So, we further optimized the r/d to 0.58.

Figure 7(c) and (d) shows the BLs and n_{eff} curves of the LP01-LP31 and CNT01 modes of the optimized r/d = 0.58 in the range of λ=1.3-1.7 μm. The n_{eff} of the optimized CNT01 mode has decrease significantly, and is only coupled with the LP31 mode at 1.31 μm where a high loss peak appears of LP31 mode as shown in Fig. 7(c). With the n_{eff} of CNT01 mode increase, the BL regions of LP02 and LP31 modes are significantly reduced compared to before. The low BL bands of LP02 and LP31 modes are increased to 1.38-1.62 μm and 1.4-1.61 μm, respectively, and the available bandwidth is increased by 60 nm compared with r/d = 0.6. In the inserted figure in Fig. 7(c), we plot the BL-Ratio curves of LP02/LP01 and LP31/LP01, respectively. The range of values 100 is 1.36-1.63 μm due to the reduction of loss. Overall, we got a 210 nm bandwidth of wavelength of 1.4-1.61 μm that the BLs are $<3.0\times10^{-4}$ dB/m by further optimizing the r/d to 0.58.

5. Discussion and summary

For the further discussion of the mode property, the proposed HC-ARF can actually support more modes when the HC-ARF is kept in straight, but the properties of bending are more attractive to us. Simulations show that only five modes can meet expectations no matter the parameters are optimized. The loss of higher order modes is about two orders higher than that of mode LP31. In addition, the HC-ARF is usually fabricated using the stack-and-draw technique. The uniform thickness of the cladding tube is the biggest challenge in the fabrication, which requires precise control of drawing tensor and pressures. Meanwhile we have chosen anti-resonance order$m$=2 to both keep relatively low loss and satisfy the fabrication feasibility.

We have proposed a novel HC-ARF with glass-sheet conjoined nested tubes which has successfully extended the HC-ARF from single-mode to few-mode in the wavelength range of 1.4-1.61 μm. The special cladding structure with conjoined nested tubes was induced to suppress the couplings between the cladding and core modes (LP01-LP31). We have optimized the parameter r/d of the proposed HC-ARF and found an operation wavelength window of low CL and CL-Ratio for few-mode transmission. The critical fiber core radius for low loss (CL$<3.0\times10^{-4}$ dB/m) and weakly modes crosstalk ($\Delta n_{eff} > 1.0\times10^{-4}$) was obtained. Simulation shows the optimized few-mode HC-ARF can support LP01-LP31 modes with low mode couplings, large DGD and extremely low CL in a large wavelength range of 1.33-1.63 μm. We also focused on the feasibility of optimizing the BL. Since the dependence of core modes and cladding modes, we changed the n_{eff} of cladding mode by decreasing conjoined nested tubes radius to suppress the coupling between core and cladding modes. It is finally achieved that the five modes of LP01-LP31 can still be transmitted with BLs are3.0×10^{-4} dB/m in the range of λ=1.4-1.61 μm at bending radius is 6 cm. The few-mode HC-ARF achieved transmission of few-mode with low loss, low nonlinear and large DGD, which could be applied to large-capacity and high-speed data transmission.

Funding. "Pioneer" and "Leading Goose" R&D Program of Zhejiang (Nos. 2022C03066, Nos. 2022C03084); National Natural Science Foundation of China (No.61775197).

Acknowledgments. This work is supported by **"**Pioneer**"** and **"**Leading Goose**"** R&D Program of Zhejiang (Nos. 2022C03084 and 2022C03066), and National Natural Science Foundation under Grant No. 61775197.

Disclosures. The authors declare no conflicts of interest.

Optics EXPRESS

Data availability. Date underlying the results presented in this paper are not publicly available at this time but may be obtained from the authors upon reasonable request.

References

1. J. C. Knight, J. Broeng, T. A. Birks, and P. S. J. Russell, "Photonic band gap guidance in optical fibers," Science **282**(5393), 1476–1478 (1998).
2. R. F. Cregan, B. J. Mangan, J. C. Knight, T. A. Birks, P. S. Russell, P. J. Roberts, and D. C. Allan, "Single-mode photonic band gap guidance of light in air," Science **285**(5433), 1537–1539 (1999).
3. F. Benabid, J. C. Knight, G. Antonopoulos, and P. S. J. Russell, "Stimulated Raman Scattering in Hydrogen-Filled Hollow-Core Photonic Crystal Fiber," Science **298**(5592), 399–402 (2002).
4. F. Yu and J. C. Knight, "Negative curvature hollow-core optical fiber," IEEE J. Sel. Top. Quantum Electron. **22**(2), 146–155 (2016).
5. S. G. Johnson, M. Ibanescu, M. Skorobogatiy, O. Weisberg, and T. D. Engeness, "Low-loss asymptotically single-mode propagation in large-core Omniguide fibers," Opt. Express **9**(13), 748–779 (2001).
6. P. St.J. Russell, "Photonic crystal fibers," Science **299**(5605), 358–362 (2003).
7. G. Pearce, G. Wiederhecker, C. Poulton, S. Burger, P. S. J. Russell, M. Soljačić, S. A. Jacobs, J. D. Joannopoulos, and Y. Fink, "Modes for guidance in kagome-structured hollow-core photonic crystal fibres," Opt. Express **15**(20), 12680–12685 (2007).
8. A. N. Kolyadin, A. F. Kosolapov, A. D. Pryamikov, A. S. Biriukov, V. G. Plotnichenko, and E. M. Dianov, "Light transmission in negative curvature hollow core fiber in extremely high material loss region," Opt. Express **21**(8), 9514–9519 (2013).
9. F. Y. u and J. C. Knight, "Spectral attenuation limits of silica hollow core negative curvature fiber," Opt. Express **21**(18), 21466–21471 (2013).
10. P. Jaworski, F. Yu, R. R. J. Maier, W. J. Wadsworth, J. C. Knight, J. D. Shephard, and D. P. Hand, "Picosecond and nanosecond pulse delivery through a hollow-core negative curvature fiber for micro-machining applications," Opt. Express **21**(19), 22742–22753 (2013).
11. M. Michieletto, J. K. Lyngs, C. Jakobsen, J. Lgsgaard, O. Bang, and T. T. Alkeskjold, "Hollow-core fibers for high power pulse delivery," Opt. Express **24**(7), 7103–7119 (2016).
12. F. Poletti, "Nested antiresonant nodeless hollow core fiber," Opt. Express **22**(20), 23807–23828 (2014).
13. C. L. Wei, R. J. Weiblen, C. R. Menyuk, and J. Hu, "Negative curvature fibers: publisher's note," Adv. Opt. Photonics **9**(3), 562 (2017).
14. M. S. Habib, O. Bang, and M. Bache, "Low-loss hollow-core silica fibers with adjacent nested anti-resonant tubes," Opt. Express **23**(13), 17394–17406 (2015).
15. W. Belardi and J. C. Knight, "Hollow antiresonant fibers with low bending loss," Opt. Express **22**(8), 10091–10096 (2014).
16. A. F. Kosolapov, G. K. Alagashev, and A. N. Kolyadin, "Hollow-core revolver fibre with a double-capillary reflective cladding," Quantum Electron. **46**(3), 267–270 (2016).
17. Z. Wang, J. J. Tu, Z. Y. Liu, C. Y. Yu, and C. Lu, "Design of weakly coupled two-mode hollow-core antiresonant fiber with low loss," J. Lightwave Technol. **38**(4), 864–874 (2020).
18. T. Bradley, G. Jasion, J. Hayes, Y. Chen, and F. Poletti, "Antiresonant hollow core fibre with 0.65 dB/km attenuation across the C and L telecommunication bands," *45th European Conference on Optical Communication (ECOC)*, 1–4 (2019).
19. G. T. Jasion, T. Bradley, K. Harringtan, H. Sakr, and F. Poletti, "Hollow core NANF with 0.28 dB/km attenuation in the C and L bands," *Optical Fiber Communications Conference and Exhibition (OFC)*, 1–3 (2020).
20. M. A. Taubenblatt, "Optical interconnects for high-performance computing," J. Lightwave Technol. **30**(4), 448–457 (2012).
21. P. J. Winzer, "Making spatial multiplexing a reality," Nat. Photonics **8**(5), 345–348 (2014).
22. D. J. Richardson, J. M. Fini, and L. E. Nelson, "Space-division multiplexing in optical fibres," Nat. Photonics **7**(5), 354–362 (2013).
23. L.Wang, S. Larochelle, "Design of eight-mode polarization-maintaining few-mode fiber for multiple-input multiple-output-free spatial division multiplexing," Opt. Letters **40**(24), 5846–5849 (2015).
24. M. S. Habib, J. E. Antonio-Lopez, C. Markos, A. Schülzgen, and R. Amezcua-Correa, "Single-mode, low loss hollow-core anti-resonant fiber designs," Opt. Express **27**(4), 3824–3836 (2019).
25. M. S. Habib, O. Bang, and M. Bache, "Low-loss single-mode hollow-core fiber with anisotropic anti-resonant elements," Opt. Express **24**(8), 8429–8436 (2016).
26. S. F. Gao, Y. Y. Wang, W. Ding, D. L. Jiang, S. Gu, X. Zhang, and P. Wang, "Hollow-core conjoined-tube negative-curvature fibre with ultralow loss," Nat. Commun. **9**(1), 2828 (2018).
27. W. Shere, G. T. Jasion, E. N. Fokoua, and F. Poletti, "Low loss, large bandwidth antiresonant hollow-core fiber design for short-reach links," OFC (2020).
28. Y. M. Jung, Q. G. Kang, H. Y. Zhou, R. Zhang, S. Chen, H. H. Wang, Y. C. Yang, X. Q. Jin, F. P. Payne, S. Alam, and D. J. Richardson, "Low-loss 25.3 km few-mode ring-core fiber for mode-division multiplexed transmission," J. Lightwave Technol. **35**(8), 1363–1368 (2017).

Optics EXPRESS

29. C. L. Wei, C. R. Menyuk, and J. T. Hu, "Impact of cladding tubes in chalcogenide negative curvature fibers," IEEE Photonics J. **8**(3), 1–9 (2016).
30. E. A. J. Marcatili and R. A. Schmeltzer, "Hollow metallic and dielectric waveguides for long distance optical transmission and lasers," The Bell Syst. Tech. J. **43**(4), 1783–1809 (1964).
31. P. Sillard, M. Bigot-Astruc, D. Boivin, H. Maerten, and L. Provost, "Few-mode fiber for uncoupled mode-division multiplexing transmissions," *2011 37th European Conference and Exhibition on Optical Communication*, 1–3 (2011).
32. M. Heiblum and J. Harris, "Analysis of curved optical waveguides by conformal transformation," IEEE J. Quantum Electron. **11**(2), 75–83 (1975).